Report for ME1500

XRD–CT Data Acquisition

Crystallographic information was obtained from the FIB machined portion of the proton irradiated $(Nb_{0.85}, Zr_{0.15})_4AlC_3$ sample through XRD – CT analysis as illustrated in figure 1a. The acquisition was performed using a 60keV X–ray beam of dimensions 0.3×0.7µm in the far field mode, at a sample to detector distance of approximately 20cm. Diffraction patterns resulting from the interaction of the beam with the sample, an example of which is displayed in figure 1b, were captured by a FReLoN 4M detector with a pixel size of 50µm. At each rotation angle ω at which the sample was placed, the rotation stage was moved so as to raster scan the beam over the sample in 0.5µm steps across a distance of 30µm in the y direction. This process was repeated at displacements of the beam relative to the sample in the z direction ranging from 0µm to 50µm beneath the sample surface. Consequently the characterisation of the sample crystal structure as a function of depth was enabled, thereby allowing conclusions to be drawn regarding the crystallographic response of the MAX phase alloy in question to proton radiation of varying doses.

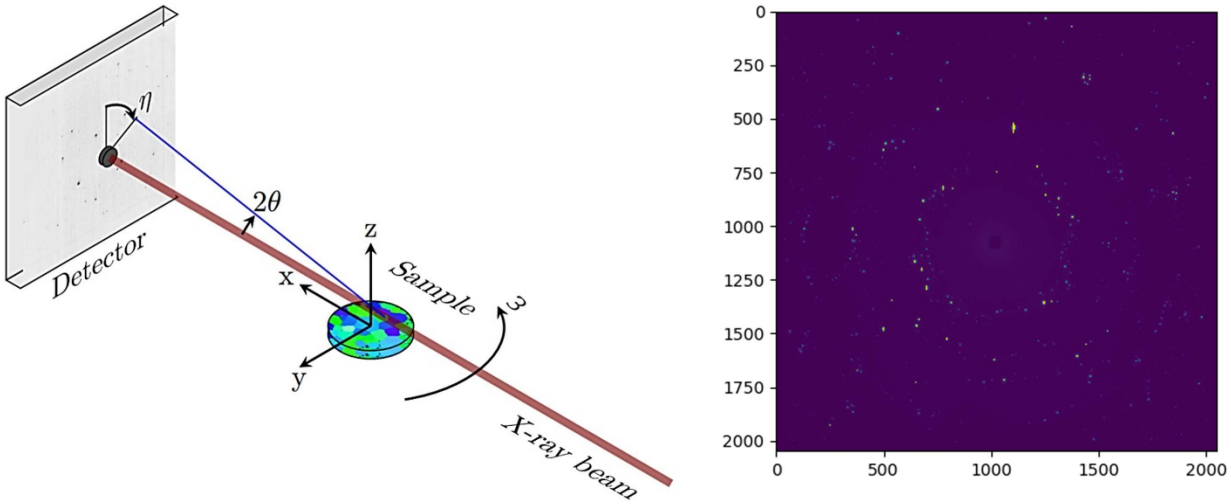

Figure 1: a) *Schematic of the XRD–CT scanning methodology employed in the acquisition at beamline ID11 of the ESRF* (Ristinmaa *et al.*, 2019). b) *Example of a diffraction pattern, showing signal from approximately 10 crystallites, captured in the experiment.*

XRD–CT Data Analysis

Analysis of the diffraction data obtained in the experiment was performed using the ImageD11 package from the Fully Automatic BeamLine Experiments (FABLE) software suite (Wright, 2008). In this analysis routine, a thresholding segmentation operation was first employed to identify connected regions of intensity corresponding to diffraction spots and separate these from the background. The cut-off intensity parameter above which all signal was considered to originate from the diffraction pattern was chosen so as to be just in excess of the background noise level. The segmented diffraction spots were subsequently matched to the diffracting grains from which they originated by means of the ImageD11 indexing procedure. In this routine, each diffraction spot was assigned a reciprocal lattice vector, G – vector, calculated by applying the treatment Busing and Levy to the 2θ and μ coordinates of the spot centre-of-mass (Busing and Levy, 1967). G – vectors were stored as $\boldsymbol{UBI}$ matrices, in accordance with the formulation of Busing and Levy, allowing conversions to be made between the reciprocal space and laboratory coordinate systems. High fidelity was ensured in the indexed grain data by removing grains of which the proportion of corresponding G – vectors with percentage errors in excess of a maximum acceptable tolerance exceeded a set ceiling value.

Grain shape reconstruction was performed through the ImageD11 implementation of the filtered back projection (FBP) method. This necessitated the construction of sinograms, consisting of indexed diffraction peak intensity as a function of y and ω, for every grain in the dataset. Grain shapes were recovered from the sinograms by application of the inverse Radon transform, with a ramp function employed to ameliorate the effects of low quality data in the periphery of the reconstructions. Obfuscation of the reconstructed grains by noise and anomalous peaks was combatted by only considering pixels to belong to a specific reconstructed grain if the corresponding pixel intensity was at least one third of the maximum intensity observed in that grain. To guarantee reasonable congruency between the reconstructed and raw data, reconstructed grains were required to achieve a correlation coefficient score of at least 0.8 with their raw counterparts in order to be accepted. Grain maps at each z depth imaged in the experiment were obtained through this reconstruction procedure. Grains were assigned *rgb* values in accordance with the corresponding inverse pole figure orientation and average grain size was determined for each map by means of the intercept method. An example grain map generated in the reconstruction process along with the accompanying inverse pole figure is given in figure 3. Also included is an illustration of the intercept method, which identified grain boundaries by locating discontinuities in *rgb* values.

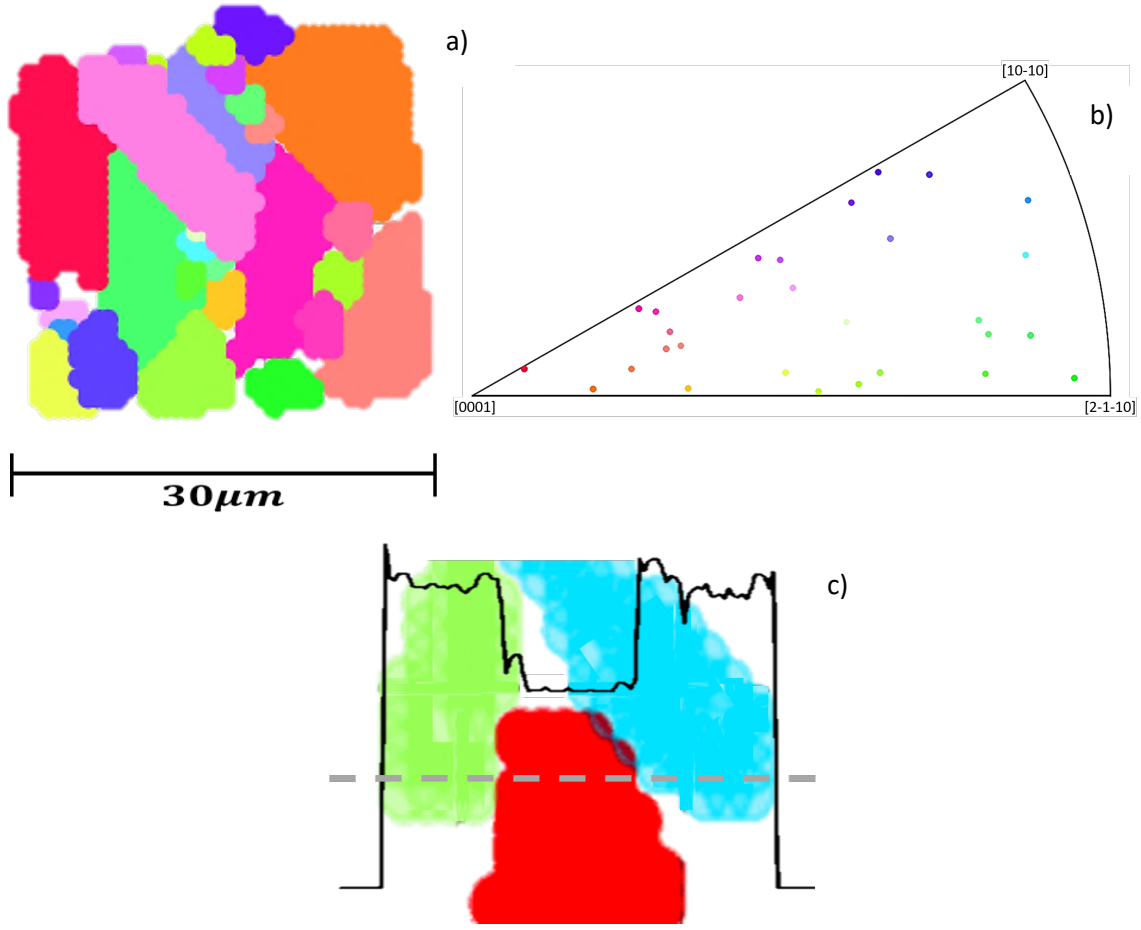

Figure 2: a) *Slice of reconstructed grains obtained in the experiment at a depth of 100μm in the sample. b) Inverse pole figure showing the correspondence of colour to grain orientation. c) Illustration of the determination of grain size by the intercept method.*